

Analysis of the X and time-resolved XUV emission of a laser produced Xe plasma

S. Bastiani-Ceccotti¹, N. Kontogiannopoulos¹, J.-R. Marques¹, S. Tzortzakis¹,

L. Lecherbourg¹, F. Thais², I. Matsushima³, O. Peyrusse⁴, and C. Chenais-Popovics¹

¹ *Laboratoire pour l'Utilisation des Lasers Intenses (LULI), UMR 7605 CNRS – CEA –
Université Paris VI – Ecole Polytechnique, 91128 Palaiseau Cedex, France*

² *CEA/DSM/SPAM, Centre d'Etudes de Saclay, 91191 Gif-sur-Yvette Cedex, France*

³ *National Institute of Advanced Industrial Science and Technology, Tsukuba, 3058568, Japan*

⁴ *CELIA, UMR 5107 Université Bordeaux 1 – CEA – CNRS, 33405 Talence, France*

Hot dense plasmas are mainly composed by multicharged ions. These ions rule the radiation transport in stellar atmospheres and in inertial fusion plasmas, and are very interesting bright X-ray sources. High-Z hot dense plasmas are usually out of local-thermodynamic-equilibrium and have to be described by sophisticated atomic physics models. Among others, the superconfiguration description of the atomic levels is very promising, but the codes still need to be benchmarked with well-diagnosed experiments. In the present experiment, time-resolved XUV spectra have been measured simultaneously with X-ray spectra, to test on a wide spectral range the predictions of the collisional-radiative, superconfiguration code AVERROES [1]. Density and temperature of the plasma were measured with Thomson scattering.

The experimental setup is shown in Fig. 1. A flat-top, 1.5 ns duration, frequency doubled neodymium laser beam ($\lambda = 0.53 \mu\text{m}$) of the LULI 2000 facility was focused on a xenon gas jet. The focalization was obtained with a $f = 800$ mm lens coupled to a random phase plate (RPP), to obtain an elliptic focal spot 1 mm large (equal to the gas jet diameter to avoid reabsorption in the cold gas) and 150 μm high (to optimize the spectral resolution of the Bragg crystal spectrograph). The laser energy was varied in the range 100 – 400 J, corresponding to $0.5 - 2 \cdot 10^{14}$ W/cm². The gas jet pressure was varied from 1.3 to 7 bar, giving an ion density in the focal volume varying linearly with the pressure from 1.7 to $9.0 \cdot 10^{18}$ cm⁻³. Laser absorption was measured with a calorimeter and found to range from 28% to 55% when the gas pressure was varied from 1.3 to 7 bar. The laser-gas interaction region was monitored with an X-ray pinhole camera. For the Thomson self-scattering diagnostic (TS), the incident laser beam scattered at 135° was collected with a $f/6$ lens. Both ionic and electronic components were recorded and time-resolved with streak cameras, with a resolution better

than 20 ps. The analysis of the spectra permit to infer the value of the product of the average charge by the electronic temperature $\langle ZT_e \rangle$, from the ionic component, and the electron density n_e from the electronic one [2]. Measurement in a fully ionized helium gas jet provided the ionic density. Then the plasma parameters n_e , n_i , $\langle Z \rangle$, and T_e were determined.

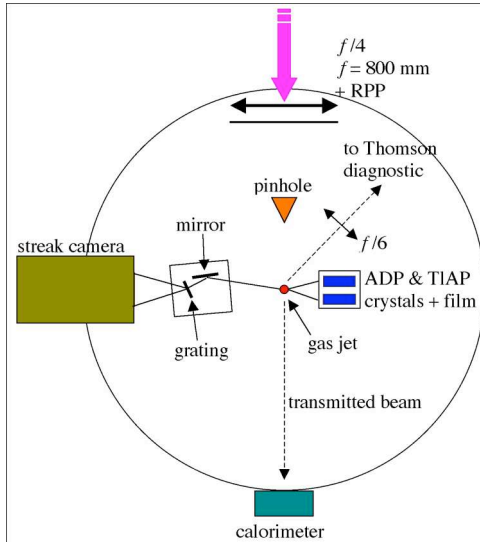


Figure 1: Experimental setup.

The analysis of the Thomson time-resolved spectra was performed with a parametric fit of the measured spectra by theoretical plots [3]. XUV spectra were measured with a 2000 l/mm transmission grating coupled to a 5 m radius spherical imaging nickel mirror. For the keV emission measurements, a TIAP Bragg crystal spectrograph equipped with DEF film was used to record the 3d-4f transitions of xenon.

For different laser energies and gas pressure, the TS diagnostic gave the following parameters: $n_e = 0.2\text{-}1.2 \cdot 10^{19} \text{ cm}^{-3}$, $\langle Z \rangle = 12\text{-}24$, $T_e = 160\text{-}500 \text{ eV}$. The time-integrated, space-resolved spectra obtained in the keV range show that the emission was homogeneous along the gas jet diameter. The spectrum is mostly composed of 3d-4f unresolved transition arrays. A lineout of the X-ray emission spectra for different gas pressure and laser energy are traced, at the center of the gas jet, in Fig. 2. The spectra are dominated by the 3d-4f transition arrays emitted by different ionic stages (Xe^{26+} to Xe^{31+}). One can observe that the transition arrays amplitude ratios follow the ionization of the gas that increases with incident laser intensity and gas pressure. Indeed, the absorbed laser energy increases with these two parameters. The spectra measured for 2 bar – 127 J and 1.3 bar – 420 J are very similar, showing that the absorbed laser energy is similar for these two different conditions. Streak images of the time-resolved XUV emission measured for 4 bar gas pressure and 360 J laser energy are shown in Fig. 3. Wavelengths were calibrated using the K-edge of beryllium and the L-edge of aluminum filters. Emission lasts longer than the 1.5 ns laser pulse. The time dependence is especially visible around 50 Å, where a bright structure disappears earlier than the rest of the spectrum. Previous calculations had shown that the xenon Co-like ions (Xe^{27+}) emit around 50 Å [4]. This highly ionized charge state disappears after 1 ns.

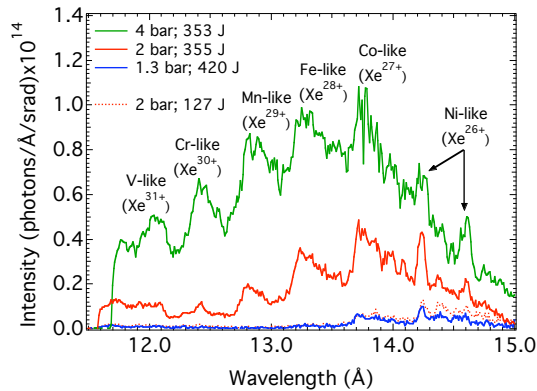


Figure 2: Xe X-ray spectra as a function of gas pressure and laser energy.

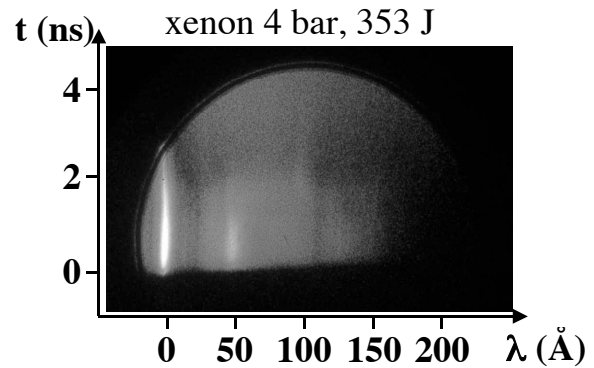


Figure 3: XUV streaked image recorded at 4 bar gas pressure. The wavelength origin is settled on the zero order.

In Fig. 4 we compare the experimental results on the XUV and the keV spectra at 2 bar gas pressure and 355 J laser energy to the calculations performed with the collisional-radiative AVERROES-TRANSPEC code. The AVERROES code generates collisional and radiative rates with the superconfiguration and supertransition arrays (STA) concept [1]. These data are then used in the population kinetics model TRANSPEC [5] to calculate the spectrum, for a given density and temperature. TRANSPEC can also be coupled as a post-processor of a hydrodynamic code.

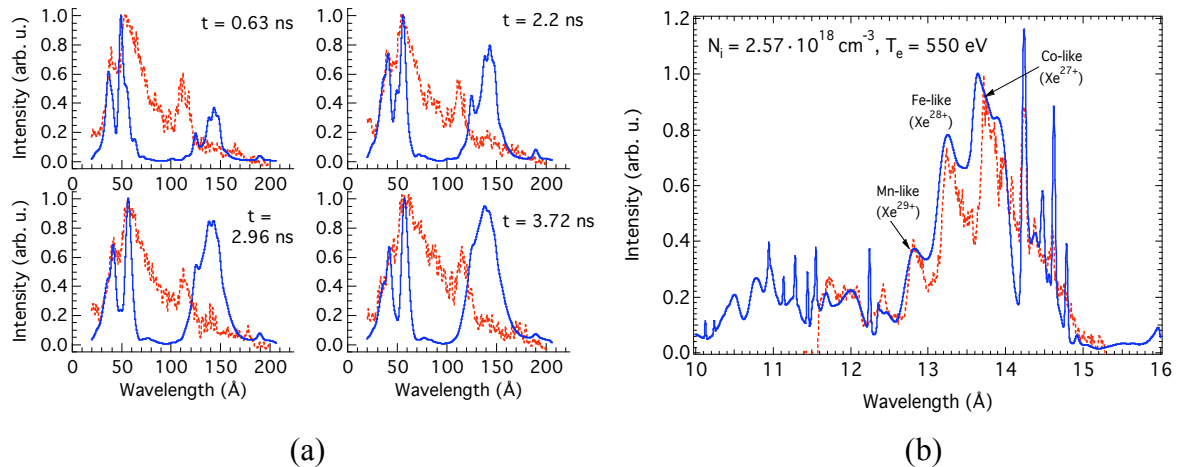


Figure 4: (see text) (a) XUV spectra at different times (dashed lines) compared with the TRANSPEC calculations (full lines) obtained with an electronic temperature of 300 eV; (b) X-ray spectrum (dashed line), compared with the TRANSPEC calculation (full line).

The calculation for the XUV emission has been performed with an ionic density of $N_i = 2.57 \cdot 10^{18} \text{ cm}^{-3}$ and an electronic temperature of 300 eV (corresponding to a mean average state $\langle Z \rangle = 21$), both given by the Thomson diagnostic. The temperature temporal profile used in the simulations was a “square” profile, with a 0.19 ns rise time, a 0.25 ns “plateau” at 300 eV, and 2 ns fall time. We can observe that the time evolution of the

emission is quite well reproduced by the calculations: the spectral structure around 50 Å, in particular, shows a good agreement with the experimental data, even in the ratio of the two peaks. Only at very early and late times, the code gives a worse agreement. Also, the spectral shift between the measured structure at 120 Å and the calculated one at 150 Å still needs investigation. For the X-ray spectrum (Fig. 4b), we can immediately see that the Z value of the TS is too low to reproduce the experimental data, which are dominated by the Co-like structures (corresponding to a $\langle Z \rangle$ of about 27). In fact, we need to adjust the temperature to fit the measured spectrum, obtaining a final value of 550 eV. The X emission is remarkably well fitted, both in the relative intensity of the spectral structures and in wavelength.

The difference in the X and XUV/TS temperatures could be due to plasma spatial inhomogeneity. Indeed, interferometric images of the focal spot obtained on a different laser source but with a similar RPP have shown the appearance of many hot spots, due to the reduced lateral heat conductivity of the gas. So, the X-rays will be emitted from the hot plasma regions, created by the hot spots, whereas the XUV emission will be emitted from the whole plasma, resulting in a spatial averaging on the temperature. The Thomson results, in good agreement with the XUV results, seem to corroborate this hypothesis, as the large detected plasma volume ($50 \times 200 \times 300 \mu\text{m}^3$) allow the same kind of spatial average on the temperature.

To have a better insight on the temporal behavior of the XUV emission, we are performing simulation using the TRANSPEC code as a post-processor of the radiative hydrocode MULTI [6]. This will allow us to have a more realistic temperature profile, which probably will improve the XUV calculation agreement with the data.

References

- [1] O. Peyrusse, *J. Phys. B* **33** (2000) 4303-4321; *J. Quant. Spectrosc. Radiat. Transfer* **71** (2001) 571-579.
- [2] E.E. Salpeter, *Phys. Rev.* **120** (1960) 1528-1535.
- [3] V. Nagels, C. Chenais-Popovics, O. Peyrusse, S. Gary, F. Girard, V. Malka, M. Rabec-Le-Gloahec, J.-C. Gauthier, *Europhysics Conf Abstracts* **28G** (2004) pp. 4.230.
- [4] V. Nagels, C. Chenais-Popovics, V. Malka, J.-C. Gauthier, A. Bachelier, and J.-F. Wyart, *Physica Scripta* **68** (2003) 233-243.
- [5] O. Peyrusse, *Phys. Fluids B* **4** (1992) 2007; *J. Quant. Spectrosc. Radiat. Transfer* **51** (1994) 281.
- [6] R. Ramis, R. Schmalz, R. Meyer-ter-Vehn, *Comput. Phys. Commun* **49**, 475 (1988).